Published in final edited form as:

Nucl Med Commun. 2015 December ; 36(12): 1174–1180. doi:10.1097/MNM.0000000000000383.

Optimizing a ^{18}F-NaF and ^{18}F-FDG cocktail for PET assessment of metastatic castration-resistant prostate cancer

Urban Simoncic[1,2], **Scott Perlman**[3,5], **Glenn Liu**[4,5], and **Robert Jeraj**[1,2,3,5]

[1]Jozef Stefan Institute, Jamova 39, SI–1000 Ljubljana, Slovenia

[2]Department of Medical Physics, University of Wisconsin – Madison, 1111 Highland Avenue, Madison, WI 53705–2275, USA

[3]Department of Radiology, University of Wisconsin – Madison, 1111 Highland Avenue, Madison, WI 53705–2275, USA

[4]Genitourinary Oncology Research Program, University of Wisconsin Carbone Cancer Center, 600 Highland Avenue, Madison, WI 53792

[5]University of Wisconsin Carbone Cancer Center, University of Wisconsin, 1111 Highland Avenue, Madison, WI 53705–2275, USA

Abstract

Background—The ^{18}F-NaF/^{18}F-FDG cocktail PET/CT imaging has been proposed for patients with osseous metastases. This work aimed to optimize the cocktail composition for patients with metastatic castrate-resistant prostate cancer (mCRPC).

Materials and methods—Study was done on 6 patients with mCRPC that had analyzed a total of 26 lesions. Patients had ^{18}F-NaF and ^{18}F-FDG injections separated in time. Dynamic PET/CT imaging recorded uptake time course for both tracers into osseous metastases. ^{18}F-NaF and ^{18}F-FDG uptakes were decoupled by kinetic analysis, which enabled calculation of ^{18}F-NaF and ^{18}F-FDG Standardized Uptake Value (SUV) images. Peak, mean and total SUVs were evaluated for both tracers and all visible lesions. The ^{18}F-NaF/^{18}F-FDG cocktail was optimized under the assumption that contribution of both tracers to the image formation should be equal. SUV images for combined ^{18}F-NaF/^{18}F-FDG cocktail PET/CT imaging were generated for cocktail compositions with ^{18}F-NaF:^{18}F-FDG ratio varying from 1:8 to 1:2.

Results—The ^{18}F-NaF peak and mean SUVs were on average 4-5 times higher than the ^{18}F-FDG peak and mean SUVs, with inter-lesion coefficient-of-variations (COV) of 20%. ^{18}F-NaF total SUV was on average 7 times higher than the ^{18}F-FDG total SUV. When the ^{18}F-NaF:^{18}F-FDG ratio changed from 1:8 to 1:2, typical SUV on generated PET images increased by 50%, while change in uptake visual pattern was hardly noticeable.

First and corresponding author: Urban Simoncic, Institute Jozef Stefan, Jamova 39, SI-1000 Ljubljana, Slovenia, urban.simoncic@ijs.si.

Conflict of Interest Notification

There are no conflicts of interests.

Conclusion—The ^{18}F-NaF/^{18}F-FDG cocktail has equal contributions of both tracers to the image formation when the ^{18}F-NaF:^{18}F-FDG ratio is 1:5. Therefore we propose this ratio as the optimal cocktail composition for mCRPC patients. We also urge to strictly control the ^{18}F-NaF/^{18}F-FDG cocktail composition in any ^{18}F-NaF/^{18}F-FDG cocktail PET/CT exams.

Keywords

^{18}F-NaF PET/CT imaging; ^{18}F-FDG PET/CT imaging; combined ^{18}F-NaF and ^{18}F-FDG cocktail PET/CT imaging; prostate cancer; osseous metastases

Introduction

Development of osseous metastases is the principal site of disease spread in cancers of the prostate, breast, lung, and kidney [1]. Detection and staging of osseous metastases is most often performed with the bone scintigraphy (BS), but positron emission tomography (PET), aided with computed tomography (CT), can provide greater sensitivity and resolution than BS. Magnetic resonance imaging (MRI) and X-ray are often used in case of equivocal findings. CT, MRI and PET are used also to detect soft tissue metastases. Despite the abundance of medical imaging modalities, no single imaging technique is optimal for all types of osseous metastases imaging.

PET imaging with various radiopharmaceuticals can provide tumour-specific or bone-specific information. The 2-[^{18}F]-fluoro-2-deoxy-D-glucose (^{18}F-FDG) is a PET marker of glucose metabolism [2], which is often increased in tumours due to Warburg effect. The sodium-[^{18}F]-fluoride (^{18}F-NaF) is a PET marker of osteoblastic activity with high potential for detecting osseous metastases [3]. In order to combine strengths of ^{18}F-FDG and ^{18}F-NaF PET/CT in osseous metastases management, the combination of ^{18}F-NaF and ^{18}F-FDG PET/CT has been assessed on preclinical cancer model, and found to improve osseous metastases detection rates [4]. Several clinical studies have found increased sensitivity of using both ^{18}F-NaF and ^{18}F-FDG PET/CT for detection of osseous metastases, when compared with separate ^{18}F-NaF PET/CT or ^{18}F-FDG PET/CT [5-7]. With the intention to make the ^{18}F-NaF and ^{18}F-FDG PET/CT more convenient, a combined ^{18}F-NaF/^{18}F-FDG cocktail PET/CT imaging approach has been demonstrated in small pilot study [8], and more thoroughly evaluated in multiple clinical studies [9-11].

Despite the demonstrated benefits of combined ^{18}F-NaF/^{18}F-FDG cocktail PET/CT imaging for the management of patients with osseous metastases, the approach has some limitations. One major limitation, which has been recognized by the authors of the studies [9-10], and further pointed out by the Invited Perspective [12] and critical responses to the first large clinical trial with ^{18}F-NaF/^{18}F-FDG cocktail PET/CT [13-14], is the sub-optimal and not strictly controlled ^{18}F-NaF/^{18}F-FDG cocktail composition. Static PET/CT imaging with ambiguouos ^{18}F-NaF/^{18}F-FDG cocktail composition is inferior because the quantification of combined ^{18}F-NaF/^{18}F-FDG PET/CT images is not possible. If the cocktail for combined ^{18}F-NaF/^{18}F-FDG imaging procedure was strictly standardized, image quantification with the Standardized Uptake Value (SUV) measure would be possible [9, 13-14]. Although the ^{18}F-FDG and ^{18}F-NaF SUV ranges from current clinical practice

cannot be directly applied for combined ^{18}F-NaF/^{18}F-FDG cocktail PET/CT imaging, the combined ^{18}F-NaF/^{18}F-FDG PET/CT images with controlled cocktail composition would be repeatable and reference SUVs would emerge with a wider adaption of such imaging in clinical practice. Obviously, the ^{18}F-NaF/^{18}F-FDG cocktail composition should be optimized before the standardization, as this could make cases with poorly visualized lesions on the combined scan less frequent [9], and potentially reduce the exposure of patients to radiation [10].

An objective of this study was to optimize the composition of the ^{18}F-NaF/^{18}F-FDG cocktail for metastatic castrate-resistant prostate cancers (mCRPC) patients, and to assess how the variation in the ^{18}F-NaF/^{18}F-FDG cocktail composition affects the combined ^{18}F-NaF/^{18}F-FDG SUV images.

Methods and materials

Patients and imaging

In this work we used clinical data from the clinical study that aimed to determine the pharmacodynamic effects of Zibotetan (ZD4054) on mCRPC patients with the various imaging tools (CT, BS, MRI, ^{18}F-NaF/^{18}F-FDG PET) [15].

The study enrolled male patients older than 18 years, with histologically proven castration resistant adenocarcinoma of prostate and at least one clinically/radiographically identified prostate metastasis in the vertebral body, pelvis or other bone that was amenable to serial imaging using PET/CT and MRI imaging. Other key inclusion criteria included the evidence of progressive disease as evident by either radiographic progression (e.g., new lesions on bone scan or new/enlarging lesions on CT scan) or a rising PSA within four weeks prior to registration (i.e., two subsequent rises in PSA measurement, each separated from the previous by a minimum of two weeks). Exclusion criteria included bilirubin above 1.5 mg/dL, SGPT (ALT) above two times the institutional upper limit of normal, creatinine above 1.5 mg/dL AND a calculated creatinine clearance below 50 mL/min, and ECOG performance status >2. A total 6 patients with median age of 68 (range, 57–88) were enrolled that provided 18 combined ^{18}F-NaF/^{18}F-FDG PET/CT imaging studies.

Patients were treated with Zibotentan (ZD4054; AstraZeneca) in six weeks cycle when the imaging was carried out (four weeks on therapy, following by two weeks of treatment break). The purpose for this dosing schedule was to allow pharmacodynamic imaging to be conducted during and after ZD4054 exposure. All subsequent cycles of therapy were four weeks in duration. Treatment continued until disease progressed, changes in the patient's condition render the patient unacceptable for further treatment or patient decided to withdraw from the study.

Patients received a combined ^{18}F-NaF/^{18}F-FDG PET/CT scans before the therapy (Baseline), at peak drug exposure (Week 4), and at maximal drug washout (Week 6). The ^{18}F-NaF/^{18}F-FDG PET/CT scanning procedure was the following: (1) patients had administered 120±15 MBq of ^{18}F-NaF while lying on the scanner table, (2) a 30 min dynamic PET acquisition started with the administration of ^{18}F-NaF over the region with the

highest suspected density of lesions, (3) a static whole body scan was acquired approximately 50 min after the administration of ^{18}F-NaF, (4) a static scan of 3 min over the same position as the ^{18}F-NaF PET/CT dynamic scan was acquired approximately 100 min after the administration of ^{18}F-NaF, (5) the ^{18}F-FDG with activity of 240±15 MBq was administrated immediately after the static scan of 3 min, and (6) a 45 min dynamic PET acquisition over the same position as the ^{18}F-NaF PET/CT dynamic scan started with the administration of ^{18}F-FDG. Four patients had dynamic PET scans of pelvic region and two of lumbar spine region.

The data was collected in the Wisconsin Institutes for Medical Research at the University of Wisconsin – Madison. All scans were acquired on the Discovery VCT PET/CT scanner (General Electric). They were acquired in a 3D acquisition mode, and reconstructed with 3D ordered-subsets expectation maximization (OSEM) algorithm. All patients signed informed consent documents approved by the Institutional Review Board at the University of Wisconsin – Madison prior to any study-related procedures.

Image analysis

All PET images that were acquired at the same day were registered rigidly, based on the CT data in order to form a combined dynamic ^{18}F-NaF/^{18}F-FDG PET/CT image. The ^{18}F-NaF part of the image (first dynamic scan, whole body scan and static 3 min scan) was analyzed for kinetics using the two-tissue compartment with four kinetic parameters and vasculature fraction [16]. The ^{18}F-NaF part of combined ^{18}F-NaF/^{18}F-FDG PET image was extrapolated by using compartmental model and estimated ^{18}F-NaF kinetic parameters, and subtracted from the combined dynamic ^{18}F-NaF/^{18}F-FDG PET image. The dynamic ^{18}F-FDG PET image, which was obtained by subtraction of ^{18}F-NaF part from combined dynamic PET image, was analyzed for kinetics using two-tissue compartment with three kinetic parameters [17]. The kinetic analysis was done on a voxel basis by using image-derived input function, which was obtained by placing the ROI on large vasculature structure (aortic arch or abdominal aorta) and taking the average time activity curve over this region. Additionally, input function was scaled with a plasma-to-whole-blood ratio of 1.2 [16, 18] for the ^{18}F-NaF and 1.0 for the ^{18}F-FDG [19]. The ^{18}F-NaF and ^{18}F-FDG SUVs at 60 min post-injection were calculated on a voxel basis using the compartmental models, input functions and estimated kinetic parameters.

All the visible suspected metastases were included in the analysis. Metastases were segmented on SUV images by a two-step process: in the first step all the suspicious regions were manually delineated. In this step a single segmentation for ^{18}F-NaF and ^{18}F-FDG SUV images for particular imaging session was created. In the second step the region with ^{18}F-NaF or ^{18}F-FDG SUV at least 50% of the maximum in the segmentation from the first step was automatically segmented. In this step separate segmentations for ^{18}F-NaF and ^{18}F-FDG images were created. Up to eight lesions were segmented on each patient with a total of 26 lesions were segmented.

From the generated SUV images and corresponding segmentations three numerical uptake measures per image were calculated; peak, mean and total SUV. Out of several possible definitions of peak SUV [20] we calculated the SUV peak as the average SUVs over the

voxels, whose centers are in the sphere with 1 cm diameter that is centred in the voxel with the highest SUV. Mean SUV was obtained by averaging the SUVs over the voxels within the corresponding lesion. Total SUV represents the total/integral uptake into the lesion, and was evaluated as the mean SUV, multiplied by the lesion segmentation volume.

The data was analyzed by the Image Analysis Center (IMAC) at the University of Wisconsin. Registration and segmentation was done with Amira software (VSG). Kinetic analysis was done with custom-developed program in Matlab (The Mathworks), that utilize a cumulative representation of the image-derived input function [21].

Optimization of ^{18}F-NaF/^{18}F-FDG cocktail composition

The main principle followed in the ^{18}F-NaF/^{18}F-FDG cocktail optimization is based on the assumption that the cocktail imaging is superior to single-tracer imaging if both cocktail components typically makes significant contribution to the image formation. Under this assumption, the cocktail composition is optimal when no cocktail component have inferior contribution to the image formation, which implies that contributions of both tracers to the image formation should be equal.

The ratio of ^{18}F-NaF and ^{18}F-FDG peak, mean or total SUV was evaluated for each lesion and each imaging session. Basic statistical parameters (minimal, maximal, mean and standard deviation) were calculated over the ratios of ^{18}F-NaF and ^{18}F-FDG SUV metrices. Based on these statistical parameters, the optimal ^{18}F-NaF/^{18}F-FDG cocktail composition was determined.

The combined cocktail ^{18}F-NaF/^{18}F-FDG PET/CT images can be quantified with a generalized concept of the SUV – the SUV is calculated by multiplying the radioactivity concentration by patient weight and divided with total administered activity of the cocktail. Such SUV is expected to be sensitive to the cocktail composition because of the uneven ^{18}F-NaF and ^{18}F-FDG avidity. This effect was demonstrated by the generation of ^{18}F-NaF/^{18}F-FDG PET/CT SUV images with the variable cocktail compositions.

Results

Comparison of ^{18}F-FDG and ^{18}F-NaF SUV images

^{18}F-FDG and ^{18}F-NaF SUV images were different in typical range of values; ^{18}F-NaF SUVs were almost five times higher than the ^{18}F-FDG SUVs. Some cases had notably different spatial patterns for both images. Two examples of ^{18}F-FDG, ^{18}F-NaF and merged ^{18}F-NaF/^{18}F-FDG SUV image with highly dislocated ^{18}F-NaF and ^{18}F-FDG uptake are in Figure 1.

The ratio of ^{18}F-NaF and ^{18}F-FDG SUVs

The ^{18}F-NaF peak and mean SUVs were on average 4-5 times higher than the ^{18}F-FDG peak and mean SUVs. Inter-lesion variations in the ^{18}F-NaF:^{18}F-FDG SUV ratio were always higher than the variations between the average ^{18}F-NaF:^{18}F-FDG ratios for peak and mean SUV, or variations between the average ^{18}F-NaF:^{18}F-FDG SUV ratios for pre- mid- and post-therapy images. ^{18}F-NaF total SUV was on average 7 times higher than the ^{18}F-

FDG total SUV. The result was different from the average ^{18}F-NaF:^{18}F-FDG ratios for peak or mean SUV by more than the inter-lesion variations in ^{18}F-NaF:^{18}F-FDG ratios for peak and mean SUV, while the inter-lesion variations in ^{18}F-NaF:^{18}F-FDG ratio for total SUV were higher than the difference between the average ^{18}F-NaF:^{18}F-FDG ratio for peak or mean SUV and the average ^{18}F-NaF:^{18}F-FDG ratio for total SUV. All ^{18}F-NaF:^{18}F-FDG SUV ratios are in Table 1.

^{18}F-NaF/^{18}F-FDG PET/CT images with variable cocktail composition

The composition of ^{18}F-NaF/^{18}F-FDG cocktail determines relative contribution of each tracer's uptake to the final image. Two examples of generated ^{18}F-NaF/^{18}F-FDG PET/CT SUV images with variable cocktail compositions are in Figure 2. When increasing the ratio of administered ^{18}F-NaF and ^{18}F-FDG from 1:8 to 1:2, typical SUV increased by 50%, while the changes in uptake visual patterns are hardly noticeable.

Discussion

Despite a number of reports of combined ^{18}F-NaF/^{18}F-FDG cocktail imaging, including an international clinical trial, the technique has not gained great clinical traction yet. Because of partial overlap of the tracers' uptakes they cannot be assessed separately from combined ^{18}F-NaF/^{18}F-FDG cocktail image, which makes image interpretation more difficult. While standardization and optimization of ^{18}F-NaF/^{18}F-FDG cocktail composition does not solve this issue, it is prerequisite for quantification of combined ^{18}F-NaF/^{18}F-FDG PET/CT images, which may help to infer pathophysiologic processes and guide response assessment based on combined ^{18}F-NaF/^{18}F-FDG PET/CT images.

Results of this study suggest that the optimal ^{18}F-NaF:^{18}F-FDG ratio is lower than used in clinical trials [8-11]. The magnitude of the ^{18}F-NaF SUV was 4-5 times higher than the magnitude of the ^{18}F-FDG SUV, while the integral ^{18}F-NaF SUV was 7 times higher than the integral ^{18}F-FDG SUV. If equal contribution of both tracers to the image formation is desired, the ratio of administered ^{18}F-NaF and ^{18}F-FDG activities should be in the range from 1:7 to 1:4, depending on whether the magnitude or integral uptake is considered. As the magnitude of radiopaharmaceuticals is more likely to be assessed, we propose the cocktail composition with the ^{18}F-NaF:^{18}F-FDG ratio of 1:5 as general rule, with the notice that the optimal ^{18}F-NaF:^{18}F-FDG ratio may be different and depends on the image interpretation technique.

The ^{18}F-NaF:^{18}F-FDG ratio of 1:5 has already been proposed as an optimal by Richmond et al. [22]. Despite the same result, our study is based on different grounds than the study by Richmond et al. [22]. Our study is based on the assumption that the cocktail PET/CT could be superior to the single-tracer PET/CT only if both cocktail components makes significant contribution to the formation of typical combined ^{18}F-NaF/^{18}F-FDG PET/CT image, which led to the requirement that uptakes of both tracers into typical lesion are equal. In contrary to that, the study by Richmond et al. aimed to concurrently optimize bone and soft tissue imaging parameters [22].

Spatial displacement of ^{18}F-NaF and ^{18}F-FDG uptakes, which we already reported [15], is highly important in the context of combined ^{18}F-NaF/^{18}F-FDG cocktail PET/CT imaging because it could alter the visual pattern of combined ^{18}F-NaF/^{18}F-FDG cocktail PET/CT image if the ^{18}F-NaF/^{18}F-FDG cocktail composition varied. However, visual patterns in Figure 2 does not change dramatically when changing the ^{18}F-NaF:^{18}F-FDG ratio from 1:8 to 1:2, eventhough the ^{18}F-NaF and ^{18}F-FDG SUV images have noticeably different patterns (Figure 1). In contrary to that, the magnitude of SUV increases by 50%. Based on that we can conclude that strict control of ^{18}F-NaF:^{18}F-FDG ratio might not be necessary if the images are evaluated visually, while it is mandatory to get the repeatable quantitative results. The ^{18}F-NaF:^{18}F-FDG ratio in the past clinical studies was not strictly controlled, most likely because ^{18}F-NaF and ^{18}F-FDG were administered separately [8-11]. If ^{18}F-NaF and ^{18}F-FDG can be mixed before the administration, the strict control of ^{18}F-NaF:^{18}F-FDG ratio would be straightforward.

This study is limited by moderate number of combined ^{18}F-NaF/^{18}F-FDG cocktail PET/CT studies with multiple studies originating from the same patients at different time points during the course of therapy. Homogeneous patient population limits the validity of study results to equivalent patients, but also reduces the uncertainty in results due to random variations in the studied population. In our case, all patients had blastic type of osseous metastases originating from mCRPC. Potential application of these results to other types of blastic metastases or to the lytic metastases is questionable due to variable ^{18}F-NaF and ^{18}F-FDG avidity of different osseous metastases. For example, the ^{18}F-FDG PET features the potential to gage response of metastases to therapy by its ability to obtain metabolic activity information in prostate cancer [23]. However, the ^{18}F-FDG PET may not be very sensitive for detecting osseous metastases originating from breast cancer with slightly higher than for prostate cancer, but still minor proportion of lytic metastases [24-25]. While possible low sensitivity of ^{18}F-FDG PET for detecting some osseous metastases might be improved by the use of integrated PET/CT scanner [26], more elegant solution is to use bone-specific ^{18}F-NaF, whose uptake represents both the increased blood flow and bone turnover characteristic of malignant lesions in bone [27].

In addition to concerns regarding the validity of presented results in other types of blastic metastases or in the lytic metastases, one could also put into question presented optimization of ^{18}F-NaF/^{18}F-FDG cocktail or even cocktail PET imaging of prostate cancer patients. For these patients, ^{18}F-NaF is effective in detecting the metastases from prostate cancer that are primarily osteoblastic, while ^{18}F-FDG shows relatively poor sensitivity compared to fluoride. Therefore, it could be argued that adding ^{18}F-FDG to ^{18}F-NaF is unlikely to provide any additional information in this type of metastases, and the proposed optimal ^{18}F-NaF:^{18}F-FDG ratio represents the ^{18}F-NaF-to-background ratio. However, FDG SUVs in metastases were well above the background as evident from two exemplary patient images shown in Figure 1.

Another obstacle towards the generalization of optimal ^{18}F-NaF:^{18}F-FDG ratio for combined ^{18}F-NaF/^{18}F-FDG cocktail PET/CT imaging is possible treatment effect on the ^{18}F-NaF or ^{18}F-FDG uptake. In our study, the average ratio of ^{18}F-NaF and ^{18}F-FDG SUV and therefore the optimal cocktail composition remained stable with therapy, despite

the correlations between the ^{18}F-NaF and ^{18}F-FDG uptake responses were not always high [15]. If more effective treatment was applied, the average ratio of ^{18}F-NaF and ^{18}F-FDG SUV throughout the therapy may not stay stable. However, some lesions have shown response on PET images despite the overall progression of disease in all the patients, so the average ratio of ^{18}F-NaF and ^{18}F-FDG SUV throughout the therapy might still not be changed significantly in the case of more effective therapy. On the other hand, stable ratio of ^{18}F-NaF and ^{18}F-FDG SUV throughout the therapy also indicates that cocktail PET imaging may not be the best approach for the treatment response assessment.

While the cocktail optimization for each clinical scenario might provide superior result due to questioned repeatability in different types of metastases and the uncertain stability of the average ratio of ^{18}F-NaF and ^{18}F-FDG SUV throughout the therapy, providing clinical data for such optimization would require significant resources. In fact, the optimization of ^{18}F-NaF/^{18}F-FDG cocktail composition could have been accomplished by the use of separately collected standard static images on sequential days, with some small, but most likely negligible additional uncertainty due to the change in patient pathophysiology between PET scans with first and second radiopharmaceutical.

Because our study has shown that the visual patterns are not particularly sensitive to the exact cocktail composition, while the uptake magnitude is sensitive, the combined ^{18}F-NaF/^{18}F-FDG cocktail PET/CT imaging may be useful even if the ^{18}F-NaF/^{18}F-FDG cocktail composition is not optimized. The composition of the ^{18}F-NaF/^{18}F-FDG cocktail should still be controlled and the ^{18}F-NaF:^{18}F-FDG ratio of 1:5 should be used, unless the newely available clinical data suggests other cocktail composition. Such combined ^{18}F-NaF/^{18}F-FDG cocktail PET/CT images can be evaluated visually, while the quantification of these images by SUV or other semiquantitative measures has to be done with great caution due to potentially suboptimal cocktail composition.

Finally, dosage of ^{18}F-NaF/^{18}F-FDG cocktail for combined PET imaging should be addressed. As critical organ for radiation exposure is the same for both radiopharmaceuticals, the recommended activity of the cocktail could be estimated from recommendations for ^{18}F-NaF and ^{18}F-FDG, added up in the same proportions as ^{18}F-NaF and ^{18}F-FDG comprise the cocktail. Based on existing recommendations (5-10 mCi for NaF and 10-20 mCi for FDG) and recommended ^{18}F-NaF:^{18}F-FDG ratio of 1:5, this would be 1.5-3 mCi for ^{18}F-NaF and 7.5-15 mCi for ^{18}F-FDG, with fixed ^{18}F-NaF: ^{18}F-FDG ratio of 1:5.

Conclusion

Based on the assumption that the ^{18}F-NaF/^{18}F-FDG cocktail for PET/CT imaging has optimal composition when the uptakes of both radiopharmaceuticals to the bone metastases are equal, we propose the ^{18}F-NaF:^{18}F-FDG ratio of 1:5 for mCRPC patients. We urge to strictly control the ^{18}F-NaF/^{18}F-FDG cocktail composition in any ^{18}F-NaF/^{18}F-FDG cocktail PET/CT exams. If the images are quantified, the cocktail composition has to be optimized for specific clinical situation. If cocktail optimization is not possible, we propose

to use the cocktail with ^{18}F-NaF:^{18}F-FDG ratio of 1:5, and evaluate the images only visually, but not quantitatively.

Acknowledgment

This study was funded by AstraZeneca. The study was performed under clinical trial registration number NCT01119118 at ClinicalTrials.gov. Additional founding was provided by NIH grant 1R01CA136927, CCSG grant P30CA014520 and Slovenian Research Agency (ARRS). The authors wish to thank the UW PET program for conducting and overseeing PET scans.

References

1. Tofe AJ, Francis MD, Harvey WJ. Correlation of neoplasms with incidence and localization of skeletal metastases: An analysis of 1,355 diphosphonate bone scans. J Nucl Med. 1975; 16:986–9. [PubMed: 810549]
2. Ido T, Wan CN, Casella V, Fowler JS, Wolf AP, Reivich M, Kuhl DE. Labeled 2-Deoxy-D-Glucose Analogs - F-18-Labeled 2-Deoxy-2-Fluoro-D-Glucose, 2-Deoxy-2-Fluoro-D-Mannose and C-14-2-Deoxy-2-Fluoro-D-Glucose. Journal of Labelled Compounds & Radiopharmaceuticals. 1978; 14:175–183.
3. Blau M, Nagler W, Bender MA. Fluorine-18: a new isotope for bone scanning. J Nucl Med. 1962; 3:332–4. [PubMed: 13869926]
4. Hsu WK, Virk MS, Feeley BT, Stout DB, Chatziioannou AF, Lieberman JR. Characterization of osteolytic, osteoblastic, and mixed lesions in a prostate cancer mouse model using 18F-FDG and 18F-fluoride PET/CT. J Nucl Med. 2008; 49:414–21. [PubMed: 18287261]
5. Jadvar H, Desai B, Ji L, Conti PS, Dorff TB, Groshen SG, Gross ME, et al. Prospective evaluation of 18F-NaF and 18F-FDG PET/CT in detection of occult metastatic disease in biochemical recurrence of prostate cancer. Clin Nucl Med. 2012; 37:637–43. [PubMed: 22691503]
6. Iagaru A, Mittra E, Dick DW, Gambhir SS. Prospective evaluation of (99m)Tc MDP scintigraphy, (18)F NaF PET/CT, and (18)F FDG PET/CT for detection of skeletal metastases. Mol Imaging Biol. 2012; 14:252–9. [PubMed: 21479710]
7. Kruger S, Buck AK, Mottaghy FM, Hasenkamp E, Pauls S, Schumann C, Wibmer T, et al. Detection of bone metastases in patients with lung cancer: 99mTc-MDP planar bone scintigraphy, 18F-fluoride PET or 18F-FDG PET/CT. Eur J Nucl Med Mol Imaging. 2009; 36:1807–12. [PubMed: 19504092]
8. Iagaru A, Mittra E, Yaghoubi SS, Dick DW, Quon A, Goris ML, Gambhir SS. Novel strategy for a cocktail 18F-fluoride and 18F-FDG PET/CT scan for evaluation of malignancy: results of the pilot-phase study. J Nucl Med. 2009; 50:501–5. [PubMed: 19289439]
9. Iagaru A, Mittra E, Mosci C, Dick DW, Sathekge M, Prakash V, Iyer V, et al. Combined 18F-fluoride and 18F-FDG PET/CT scanning for evaluation of malignancy: results of an international multicenter trial. J Nucl Med. 2013; 54:176–83. [PubMed: 23243299]
10. Lin FI, Rao JE, Mittra ES, Nallapareddy K, Chengapa A, Dick DW, Gambhir SS, et al. Prospective comparison of combined 18F-FDG and 18F-NaF PET/CT vs. 18F-FDG PET/CT imaging for detection of malignancy. Eur J Nucl Med Mol Imaging. 2012; 39:262–70. [PubMed: 22065013]
11. Harisankar CN, Agrawal K, Bhattacharya A, Mittal BR. F-18 fluoro-deoxy-glucose and F-18 sodium fluoride cocktail PET/CT scan in patients with breast cancer having equivocal bone SPECT/CT. Indian J Nucl Med. 2014; 29:81–6. [PubMed: 24761058]
12. Cook GJ. Combined 18F-Fluoride and 18F-FDG PET/CT scanning for evaluation of malignancy: results of an international multicenter trial. J Nucl Med. 2013; 54:173–5. [PubMed: 23287576]
13. Cheng G, Kwee TC, Basu S, Alavi A. Critical considerations on the combined use of (1)(8)F-FDG and (1)(8)F-fluoride for PET assessment of metastatic bone disease. Eur J Nucl Med Mol Imaging. 2013; 40:1141–5. [PubMed: 23695838]
14. Niederkohr RD. Technical feasibility vs. clinical utility: a question of “can we?” vs. “should we?”. Eur J Nucl Med Mol Imaging. 2012; 39:260–1. [PubMed: 22160199]

15. Simoncic U, Perlman S, Liu G, Staab MJ, Straus JE, Jeraj R. Comparison of NaF and FDG PET/CT for Assessment of Treatment Response in Castration-Resistant Prostate Cancers With Osseous Metastases. Clin Genitourin Cancer. 2014

16. Hawkins RA, Choi Y, Huang SC, Hoh CK, Dahlbom M, Schiepers C, Satyamurthy N, et al. Evaluation of the skeletal kinetics of fluorine-18-fluoride ion with PET. J Nucl Med. 1992; 33:633–42. [PubMed: 1569473]

17. Sokoloff L, Reivich M, Kennedy C, Des Rosiers MH, Patlak CS, Pettigrew KD, Sakurada O, et al. The [14C]deoxyglucose method for the measurement of local cerebral glucose utilization: theory, procedure, and normal values in the conscious and anesthetized albino rat. J Neurochem. 1977; 28:897–916. [PubMed: 864466]

18. Doot RK, Muzi M, Peterson LM, Schubert EK, Gralow JR, Specht JM, Mankoff DA. Kinetic analysis of 18F-fluoride PET images of breast cancer bone metastases. J Nucl Med. 2010; 51:521–7. [PubMed: 20237040]

19. Gambhir SS, Schwaiger M, Huang SC, Krivokapich J, Schelbert HR, Nienaber CA, Phelps ME. Simple noninvasive quantification method for measuring myocardial glucose utilization in humans employing positron emission tomography and fluorine-18 deoxyglucose. J Nucl Med. 1989; 30:359–66. [PubMed: 2786939]

20. Vanderhoek M, Perlman SB, Jeraj R. Impact of the definition of peak standardized uptake value on quantification of treatment response. J Nucl Med. 2012; 53:4–11. [PubMed: 22213818]

21. Simoncic U, Jeraj R. Cumulative input function method for linear compartmental models and spectral analysis in PET. J Cereb Blood Flow Metab. 2011; 31:750–6. [PubMed: 20808319]

22. Richmond K, McLean N, Rold T, Szczodroski A, Dresser T, Hoffman T. Optimizing a F-18 NaF and FDG cocktail as a preclinical cancer screening tool for molecular imaging [abstract]. J Nucl Med. 2011; 52:2455.

23. Morris MJ, Akhurst T, Larson SM, Ditullio M, Chu E, Siedlecki K, Verbel D, et al. Fluorodeoxyglucose positron emission tomography as an outcome measure for castrate metastatic prostate cancer treated with antimicrotubule chemotherapy. Clin Cancer Res. 2005; 11:3210–6. [PubMed: 15867215]

24. Gallowitsch HJ, Kresnik E, Gasser J, Kumnig G, Igerc I, Mikosch P, Lind P. F-18 fluorodeoxyglucose positron-emission tomography in the diagnosis of tumor recurrence and metastases in the follow-up of patients with breast carcinoma: a comparison to conventional imaging. Invest Radiol. 2003; 38:250–6. [PubMed: 12750613]

25. Cook GJ, Houston S, Rubens R, Maisey MN, Fogelman I. Detection of bone metastases in breast cancer by 18FDG PET: differing metabolic activity in osteoblastic and osteolytic lesions. J Clin Oncol. 1998; 16:3375–9. [PubMed: 9779715]

26. Morris PG, Lynch C, Feeney JN, Patil S, Howard J, Larson SM, Dickler M, et al. Integrated Positron Emission Tomography/Computed Tomography May Render Bone Scintigraphy Unnecessary to Investigate Suspected Metastatic Breast Cancer. Journal of Clinical Oncology. 2010; 28:3154–3159. [PubMed: 20516453]

27. Even-Sapir E, Metser U, Mishani E, Lievshitz G, Lerman H, Leibovitch I. The detection of bone metastases in patients with high-risk prostate cancer: 99mTc-MDP Planar bone scintigraphy, single- and multi-field-of-view SPECT, 18F-fluoride PET, and 18F-fluoride PET/CT. J Nucl Med. 2006; 47:287–97. [PubMed: 16455635]

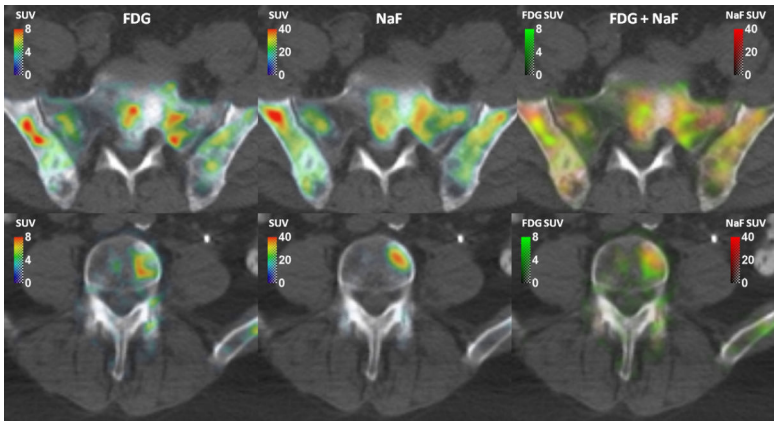

Figure 1.
Two examples of FDG SUV, NaF SUV and merged FDG/NaF SUV images.

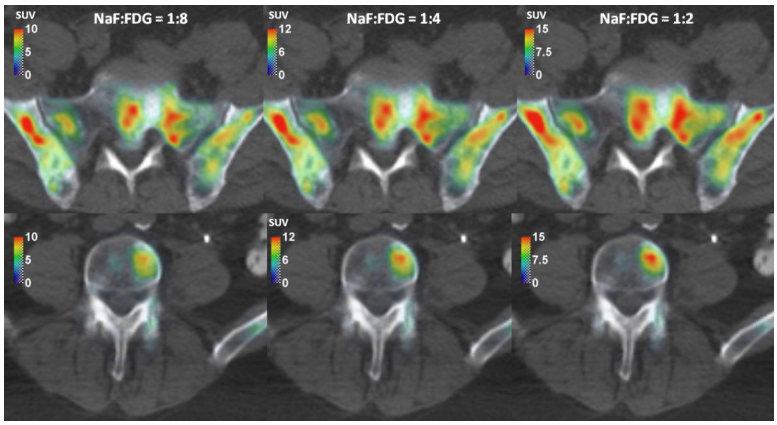

Figure 2.
The NaF/FDG cocktail PET/CT images with various NaF:FDG compositions.

Table 1

NaF:FDG SUV ratios, evaluated for Baseline (BL), Week 4 (W4) and Week 6 (W6) sessions, and all segmented lesions.

		peak SUV ratio			mean SUV ratio			total SUV ratio		
Patient	**Lesion**	**BL**	**W4**	**W6**	**BL**	**W4**	**W6**	**BL**	**W4**	**W6**
1	L ilium	4.5	3.4	4.5	3.9	3.6	4.0	12.6	9.2	8.1
	R ilium	5.6	4.1	5.8	5.2	4.0	5.9	8.6	11.1	6.9
	sacrum	5.5	4.5	5.0	5.2	4.3	4.5	5.8	7.1	5.8
	L ilium	5.1	4.4	4.8	4.5	4.3	4.2	12.4	6.7	8.8
	R ilium	4.8	4.8	4.9	4.6	4.3	5.0	5.7	8.7	4.5
	sacrum	4.9	3.9	3.7	4.8	3.8	3.7	9.4	5.7	9.5
	sacrum	5.8	4.7	5.8	5.7	5.0	5.6	10.7	9.6	9.0
2	vertebra	4.4	4.7	4.5	4.1	4.7	4.6	6.5	5.9	3.2
	R ilium	3.1	3.0	3.7	4.1	3.1	3.8	3.2	2.7	3.8
	vertebra	5.4	6.6	5.9	5.0	6.2	4.8	6.0	7.2	6.4
	vertebra	4.9	4.8	4.1	4.7	4.6	3.8	4.1	5.1	4.1
	vertebra	4.5	5.7	4.8	4.8	6.0	4.7	4.8	4.9	4.7
	vertebra	4.3	5.4	3.9	4.4	6.3	4.6	5.7	4.2	3.6
3	R ilium	3.8	3.4	4.0	3.8	2.9	3.5	2.2	7.9	3.7
	L ilium	3.7	5.7	2.3	3.6	4.3	2.2	4.3	4.5	7.1
	sacrum	3.5	4.2	3.8	3.2	4.1	4.0	6.8	6.6	3.1
	R ilium	4.1	4.3	3.9	3.9	4.1	3.7	5.5	6.5	6.2
	L ilium	3.7	5.0	5.1	3.5	4.7	4.3	6.2	8.1	4.5
	L ilium	5.9	6.5	4.6	5.2	5.4	4.1	7.9	14.5	8.6
	R ilium	4.1	4.6	4.4	4.4	3.1	4.0	4.2	16.6	5.2
	vertebra	4.7	4.6	5.8	4.7	3.8	4.8	5.9	6.9	5.9
4	sacrum	2.8	5.9	5.4	2.2	4.6	4.4	6.3	10.7	10.1
5	hip	5.2	7.1	3.9	3.7	5.8	3.2	13.6	16.5	7.6
6	vertebra	4.3	3.4	3.3	3.9	3.2	2.7	6.6	5.0	5.5

		peak SUV ratio			mean SUV ratio			total SUV ratio		
Patient	**Lesion**	**BL**	**W4**	**W6**	**BL**	**W4**	**W6**	**BL**	**W4**	**W6**
	vertebra	2.9	1.6	1.7	3.0	1.4	1.5	2.7	2.3	2.1
	vertebra	3.8	4.2	2.0	3.5	3.8	2.0	5.6	3.3	3.9
ALL	min	2.8	1.6	1.7	2.2	1.4	1.5	2.2	2.3	2.1
	max	5.9	7.1	5.9	5.7	6.3	5.9	13.6	16.6	10.1
	mean	**4.4**	**4.6**	**4.3**	**4.2**	**4.3**	**4.0**	**6.7**	**7.6**	**5.8**
	STD	0.9	1.2	1.1	0.8	1.1	1.0	3.0	3.8	2.2